

A universal and facile approach for building multifunctional conjugated polymers for human-integrated electronics

Nan Li,¹ Yahao Dai,¹ Yang Li,¹ Shilei Dai,¹ Joseph Strzalka,² Qi Su,¹ Nickolas De Oliveira,¹ Qingteng Zhang,² P. Blake J. St. Onge,³ Simon Rondeau-Gagné,³ Yunfei Wang,⁴ Xiaodan Gu,⁴ Jie Xu,⁵ Sihong Wang^{1,6*}

¹Pritzker School of Molecular Engineering, The University of Chicago, Chicago, IL 60637, USA

²X-Ray Science Division, Argonne National Laboratory, Lemont, IL 60439, USA

³Department of Chemistry and Biochemistry, University of Windsor, Windsor, Ontario N9B3P4, Canada

⁴School of Polymer Science and Engineering, University of Southern Mississippi, Hattiesburg, MS 39406, USA

⁵Nanoscience and Technology Division, Argonne National Laboratory, Lemont, IL 60439, USA

⁶Lead Contact

*Correspondence: sihongwang@uchicago.edu

Summary

Polymer semiconductors have shown distinct promise for the development of human-integrated electronics, owing to their solution processability and mechanical softness. However, numerous functional properties required for this application domain face synthetic challenges to be imparted onto conjugated polymers and thus combined with efficient charge-transport property. Here, we develop a “click-to-polymer” (CLIP) synthesis strategy for conjugated polymers, which uses a click reaction for the facile and versatile attachment of diverse types of functional units to a pre-synthesized conjugated-polymer precursor. With four types of functional groups, we show that functionalized polymers from this CLIP method can still retain good charge-carrier mobility. We take two realized polymers to showcase the photo-patternable property and biochemical sensing function, both of which advance the

state of the art of realizing these two types of functions on conjugated polymers. We expect the expanded use of this synthesis approach can largely enrich the functional properties from conjugated polymers.

Introduction

Conjugated polymers, which feature mechanical softness and solution processability, have received substantial developments for several types of electronic devices, including organic field-effect transistors (OFETs),¹ organic photovoltaics (OPVs),² organic light-emitting diodes (OLEDs),³ and electrochromic devices.⁴ Their functional performances have already been made on par with inorganic materials. More recently, conjugated polymers have been demonstrated as the only class of electronic materials that can provide skin-like stretchability,⁵⁻⁹ thereby rendering them prime candidates for human-integrated electronics for health monitoring, disease diagnosis, and medical treatments.¹⁰⁻¹³ However, towards realizing such applications of collecting and delivering various types of information from/to human bodies, there have rarely been the designs of conjugated polymers for providing a number of emerging functions, which include, but not limited to, biochemical sensing, chemotherapeutic property, bio/immune-compatibility, micro-patternability, tissue/skin adhesion, stimuli-responsiveness. Currently, the absence of these functional properties poses the major obstacle for taking advantage of the unique properties of conjugated polymers to benefit the development of human-integrated electronics.

As these functional properties are typically afforded by certain functional units, such as bioreceptors, drug motifs, antifouling groups, and photo/thermo-reactive groups, respectively, the most straightforward and effective approach for building these functions into conjugated polymers should be to incorporate these functional units into the molecular designs, such as on the side chains. However, significant challenges arise in the synthesis of these types of molecular structures following the conventional procedure (Figure 1A) of first incorporating desired functional units

during the monomer synthesis and then carrying out the polymerization reaction at the end.¹⁴⁻¹⁸ Since many functional units of the above listed types are either highly sensitive to harsh conditions such as high temperature, high pressure and toxic reagents, or tend to significantly change a monomer's solubility, their attachment on a conjugated monomer either cannot survive through the polymerization reaction or would largely decrease the efficacy of the polymerization. For other functional units that could be compatible with this synthesis procedure, they each require unique design and optimization of the synthesis conditions, which further elevates the technical barrier. So far, the successes along this line for conjugated polymers have only been achieved on a limited number of functional groups of the above-listed types, for example, lysine groups for enhancing cell viability,¹⁴ and photochromic groups for optically tunable electrical performance.¹⁹

Alternatively, surface modification on a pre-deposited thin film of conjugated polymers presents another option for incorporating a type of function that mainly relies on surface properties, e.g., chemical sensing, biocompatibility, and adhesion. However, with the lack of suitable reactive sites in the typical designs of conjugated polymers, the viable methods are mostly limited to physical approaches such as coating or adsorption,^{20,21} which are only applicable to a small portion of functional groups and typically result in poor stability. For the generally preferred modification through covalent assembly, additional pre-treatments (e.g., oxygen plasma activation) to the film surface are often needed for generating reactive groups,²²⁻²⁵ which usually cause undesired side reactions or even degradation to conjugated polymers.

Therefore, to unlock a broad range of desired functionalities for conjugated polymers, it is highly necessary to develop a different synthesis approach that can fully decouple the covalent attachment of functional units with the polymerization reaction. Herein, we report a generalizable molecular design and synthesis approach of using click chemistry as a post-polymerization step to versatilely graft a variety of functional units onto the side chains of high-performance donor-acceptor type semiconducting conjugated polymers^{1,18} (Figure 1B), which we name as the CLick-

to-Polymer (CLIP) method. Specifically, with the criteria of having high reaction efficacy, sufficient compatibility of the clickable site with the cross-coupling (e.g., Stille-coupling) polymerization for donor-acceptor conjugated polymers, a simple reaction procedure, and minimal influence on the charge-carrier transport, we rationally choose the copper-catalyzed azide-alkyne cycloaddition (CuAAC)^{26,27} as the click reaction for the CLIP method. To the best of our knowledge, the CuAAC reaction so far has neither been used for the functionalization of a donor-acceptor conjugated polymer, nor achieved high-performance semiconducting property through considering the structure-property relationships²⁸⁻³¹. Moreover, we hypothesize that the high efficacy and the broad tunable space of the reaction condition of this click chemistry could also allow the versatile use of the CLIP for not only bulk functionalization and but also surface functionalization, by simply swapping the sequence of the click reaction and the thin-film deposition (Figure 1C), which, to the best of our knowledge, has never been reported before on a single method. This will provide the freedom of choosing the most suitable functionalization approach from the combined considerations of both the nature of the targeted function and the preservation of the electrical performance.

In this work, we demonstrated the versatility of this approach on four types of functional groups (Figure 1B, bottom) with photo-crosslinkable,³² bio-conjugation,³³ immune-modulatory,³⁴ and ionic conducting³⁵ properties, respectively. From the synthetic perspective, they covered the challenging characteristics of thermal reactivity, solvent incompatibility, and sized volume, as well as serving to solve the challenge from less stable biochemical units. The obtained conjugated polymers with the bulk functionalization of these units still give largely-preserved charge-carrier mobility (above $0.1 \text{ cm}^2 \text{ V}^{-1} \text{ s}^{-1}$ from three of the four functionalized polymers), while the surface functionalization does not cause any influence on the mobility. To demonstrate the usefulness of this CLIP strategy, we realized two highly desired functions on conjugated polymers: the direct photo-patterning with sub-10 μm resolution enabled by the incorporation of benzophenone groups;

and the amplified biomolecular sensing enabled by the incorporation of *N*-hydroxysuccinimide (NHS) ester that can conjugate with enzymatic bioreceptors. Moving forward, we envision that the further expansion of our CLIP synthesis approach to the incorporation of a large variety of functional units, such as therapeutic motifs and diverse groups of biomolecules, can greatly enrich the functions and applications of conjugated polymers for human-integrated wearable and implantable electronics.

Results and discussion

In our proposed CLIP method, the first key step is to attach the azide group onto the side chains of conjugated monomers (e.g., the acceptor units for the synthesis of donor-acceptor polymers, as shown in Figure 1B, top) during the monomer synthesis process, which serves as the click site for the later CuAAC reaction with a functional group modified with the alkyne group. For most types of functional groups, such alkyne modification can be achieved under compatible, mild conditions.³⁶⁻⁴⁰ To reduce potentially unfavorable influences of bulky functional groups on the packing structure of conjugated polymers, we introduced a linear alkyl linker between the clickable site and the backbone. Since the azide group will neither be activated (Figure S1 and S2) under the typical conditions of the polymerization reaction (e.g., the Stille-coupling reaction with the temperature range of 180-200 °C), nor influence the monomer's solubility, the subsequent polymerization can still be carried out as usual.

Bulk functionalization on conjugated polymers through the CLIP method.

With the donor-acceptor backbone of diketopyrrolopyrrole-thieno[3,2-*b*]thiophene (DPPTT) used as the model system, we first demonstrate the bulk functionalization process and characterize the obtained polymers. We synthesized DPP monomers (Figure 2A) with azide-substituted side chains in two different alkyl-linker lengths—six and ten carbons, which were further taken to copolymerize with DPP units of conventional branched alkyl side chains in two ratios of 1:9 and 2:8.

The reason of copolymerization with branched alkyl chains is to balance the desired functionality and the good solution-processability of the modified polymers. It should be noted that by adding some solubilizing side chains onto the donor (TT) units, the fraction of the functionalized DPP units could be further increased while still keeping sufficient solubility. Through the same polymerization condition, the four types of azide-substituted polymers, namely C6-10a (i.e., six-carbon alkyl linker and 10 % azide-substituted DPP units), C6-20a, C10-10a, C10-20a, all have lower molecular weights than the DPPTT polymer only with branched alkyl side chains (Table S1), which should come from the slight decrease in the solubility caused by the partial replacement of branched side chains with linear side chains. Subsequently, the four types of functional units as shown in Figure 1B, i.e., tetrahydropyran (PY), poly(ethylene glycol) 5-*N*-hydroxysuccinimide ester (PEG5NHS), benzophenone (BP), and poly(ethylene glycol)-2000-kDa (PEG2000), were grafted onto the polymers via the CuAAC click reaction. The successes of our CLIP method were verified by nuclear magnetic resonance (NMR, Figure 2B) and Fourier-transform infrared spectroscopy (FTIR, Figure S3) results, which all clearly show the existence of the azide groups after the polymerization reaction, and the subsequent disappearance of the azide after the click reaction.

To evaluate the influence of side-chain functionalization made by the CLIP method on the polymers' electrical performance, we fabricated thin-film transistor (TFT) devices to characterize the charge-carrier mobility, which are in the bottom-gate bottom-contact device structure with SiO₂/n⁺⁺-Si as the gate dielectric and gate electrodes, and gold as the source/drain electrodes (Figure 2C). In general, all the obtained polymers give ideal transfer and output characteristics (Figure S4-5), as represented by the polymer with PY-functionalization on C10-10a (Figure 2D-E). Compared to the unfunctionalized DPPTT polymer with 100 % branched-alkyl side chains, there is only some minor decrease in mobilities (Figure 2F-I and S6, Table S2-3) resulting from the side-chain modifications with the azide group alone and the four types of functional units. Such changes in mobility could be the combined effects of the changes in the packing structure, the molecular weight,

and the deposited film morphology. The extent of such influences is dictated by both the side-chain structure (i.e., the alkyl-breaker length) and the molar ratio in the co-polymerization. As shown in Figure 2F, the CLIP of the functional group PY on C10-10a results in slightly less decrease in mobility than on C6-10a. From Figure 2G and 2H, the longer alkyl linker (C10 vs C6) reduces the steric hindrance from the functional group to the polymers' packing ordering, as shown by the crystallinities measured from grazing incidence X-ray diffraction (GIXD) and aggregation level characterized by ultraviolet-visible (UV-Vis) (Figure 2G-H and S7). For the C10 polymers, on the other hand, the increase of the functionalization ratio from 10 % to 20 % (i.e., the resulted polymer of C10-20PY) leads to lower mobility (Figure 2F), which should also come from the elevated disruption to the packing structure. Besides, the decreased molecular weights of the functionalized polymers could also be a reason for the decrease in mobility,⁴¹ which in the future could be improved by enhancing the solubility of the monomers and resulted polymers through introducing additional solubilizing groups to the backbone.⁴²

The further expanded comparison of the other three types of functional groups, i.e., namely PEG5NHS, BP and PEG2000, together with PY, functionalized on C10-10a polymer all achieve mobility above $0.1 \text{ cm}^2 \text{ V}^{-1} \text{ s}^{-1}$ except PEG2000 (Figure 2I). In general, the primary influence from the types of functional group should be the different steric hindrance effects in disrupting the packing structure (Figure 2J and S8). Expectedly, PEG2000 as the bulkiest group results in the most substantial decrease in mobility. Moreover, it is observed that the functionalization overall leads to increased surface roughness of the deposited thin film as compared to C10-10a (Figure 2K and S9), which could be another factor causing the slight decrease of mobilities. Overall, benefiting from the minimal influence on the polymerization efficacy and the tunability of the side-chain structure, the functionalization to conjugated polymers using the CLIP method can largely preserve the electrical performance.

To demonstrate the unprecedented synthesis capability given by the CLIP strategy, we made

an experimental comparison to the use of the conventional pre-polymerization functionalization approach for the synthesis of the 10PEG2000 polymer, in which the PEG2000 unit is first grafted onto the DPP monomers prior to the polymerization. With such a functionalized monomer, the obtained polymer from the same Stille-coupling reaction indeed has a much lower molecular weight, together with a very low mobility around $0.001 \text{ cm}^2 \text{ V}^{-1} \text{ s}^{-1}$ (Figure S10), which should come from the substantial decrease of the reactivity of the functionalized DPP monomer as a result of the substitution of such a bulky and polar group. This comparison clearly shows that the CLIP method provides the unparalleled capability in functionalizing conjugated polymers without affecting the synthesis outcomes.

Surface functionalization on conjugated polymers through the CLIP method.

Compared to the bulk functionalization, the surface functionalization on a pre-deposited thin film can avoid the disruption to the polymer's packing structures by sizable functional groups. For enabling the CuAAC click reaction on such surfaces, the azide groups as the clickable sites need to be effectively exposed on the surfaces, which is indeed satisfied by the edge-on packing orientation (Figure S7) of the deposited C10-10a and C10-20a films. However, with the much lower amount of the azide group available on the surface as compared to that from the fully solubilized polymers, sufficiently high reaction efficiency is highly needed. For this, we chose *N,N*-dimethyl formamide (DMF) as the solvent for the click reaction, which offers good wettability to these conjugated polymer films, thus facilitating the transport of the reactant molecules to the surface. Under this condition, we carried out the surface functionalization on a C10-10a film with the unit of PEG2000. After the reaction at room temperature overnight followed by a thorough rinse to fully remove the excess reagents, we observed a decrease of the water contact angle from 98° to 67° , which suggests the successful grafting of the PEG2000 chain (Figure 3B and S11). This was further verified through the X-ray photoelectron spectroscopy (XPS) characterization, which shows the appearance of the C 1s peak (Figure 3C) and the increased intensity of the O 1s peak (Figure S12),

both corresponding to the formed C-O bond. To further exclude the possibility of physical absorption, a control experiment was carried out with the same reaction condition but without the catalyst for the click reaction, which gave little change in the contact angle or the XPS spectrum. The measurement of its charge-carrier mobility in OTFTs indeed proves that such surface functionalization causes negligible influence on the electrical performance (Figure 3D and S13), so that the mobility is almost one order of magnitude higher than that from its bulk-functionalized counterpart.

Direct photo-patterning of conjugated polymers enabled by the functionalization of benzophenone group.

Among the four types of functional units incorporated in this work, the benzophenone group can enable interchain crosslinking (Figure 4A) for the functionalized conjugated polymer through the photo-initiated reaction with an adjacently-located C-H bond⁴³ (Figure 4B) under mild-UV (365 nm) exposure. This will impart solvent resistance to pre-annealed (at 140 °C for 30 min) 10BP films when the UV exposure time is longer than 5 minutes (under the 365-nm wavelength and 2.6-mW/cm² intensity), as verified by the immersion test in chloroform (Figure S14). This could thus enable one-step direct photolithography for the patterning of the conjugated polymer film, by using a photomask to limit the UV exposure to selected areas. As conjugated polymers are generally not compatible with the solvents of normal photoresists and developers, their patterning into small feature sizes has been one of the major challenges for using them to fabricate functional circuits. Among all the potential options, the direct photo-patterning through imparting a conjugated polymer with photo-crosslinkable property is the most ideal choice for the simplicity in fabrication. So far, the very few reports about the direct photo-patterning of a semiconducting polymer are through the use of azide crosslinking reaction, by either blending an azide-containing crosslinker⁴⁴ (e.g., bis(fluorophenyl azide)) or attaching the azide group onto the polymer side chain.^{45,46} However, since the azide crosslinking chemistry requires the use of deep-UV light (i.e., with the

wavelength of 254 nm) and a relatively high exposure dose, detrimental effects could be caused for conjugated polymers, as verified by the UV-exposure experiment on our C10-10a polymer that also has the azide group (Figure S15). Alternatively, the benzophenone photo-crosslinking chemistry that is incorporated to conjugated polymers for the first time should be more benign for preserving the electrical performance after the direct photo-patterning.

We then carried out a systematic study of the crosslinking conditions to realize the full preservation of electrical performance from 10BP films after the direct photolithography process. Through testing varied UV exposure durations all followed by a post-bake step (at 170 °C for 30 min) to fully remove the development solvent (i.e., chloroform) from the film, we found that a UV exposure time equal or longer than 10 min can ensure the full preservation of the charge-carrier mobility (Figure 4C and S16) after the solvent removal of the unexposed areas. Consequently, the mobility of $\sim 0.2 \text{ cm}^2 \text{ V}^{-1} \text{ s}^{-1}$ is obtained from the patterned films of conjugated polymers. Under this photo-patterning condition, we further demonstrated the transfer of pre-designed patterns from masks to 10BP films through the one-step photolithographic process, which can indeed work well for complicated geometries and achieve a resolution below 10 μm (Figure 4D-E and S17). It can be envisaged that this CLIP-based incorporation of benzophenone group can be adopted to other designs of conjugated polymers, so as to obtain photo-patternable polymer semiconductors with even higher mobility.

Biochemical sensing enabled by the immobilization of an enzymatic bioreceptor.

The NHS ester, another group that gets functionalized onto conjugated polymers using the CLIP method, can serve to impart conjugated polymers with selective sensing to targeted biomolecules, through having the bio-conjugation reaction with the primary amine group in protein/polypeptide-type bioreceptors. Since biochemical sensing is one of the major approaches for health monitoring and disease diagnosis, imparting such functions to conjugated polymers is

highly desirable for their use in human-integrated electronics. So far, although there have been a few examples of using conjugated polymers as the channel layer in transistor-type sensors that can uniquely offer built-in amplifications for achieving higher sensitivity, the specificity was imparted by either non-covalent physical absorption method,²⁰ which lacks the long-term robustness; or through complicated surface treatment methods^{47,48} such as templating and plasma deposition, which are only applicable to a narrow range of bioreceptors.

To demonstrate this biochemical sensing function offered by the functionalized NHS ester group, we chose to immobilize the glucose oxidase (GO) enzyme as the bioreceptor for the sensing of glucose. Recently, based on the mixed electronic-ionic conducting property of conjugated polymers, organic electrochemical transistors (OECTs) have been developed as a very promising device platform for biosensing, which can provide even higher amplification to sensing signals than normal field-effect transistors.⁴⁹⁻⁵¹ In order to adopt the functionalization of NHS ester group to conjugated polymers for OECT operations, we copolymerized the azide-attached DPP monomer with the glycolated 2,2'-bithiophene (g2T) monomer,^{52,53} in the ratio of 1 to 9 (Figure S18), so as to achieve the desired ionization potential and aqueous-swelling property for OECT operation. Using this polymer, namely g2T-NHS, the glucose sensor was fabricated (Figure 5B) through first depositing the semiconducting film onto patterned gold source/drain electrodes on a glass substrate, and then treating the channel area with the solution of GO enzyme for 2 hours to achieve the covalent immobilization of this bioreceptor. The gating is made with the extended configuration of having another piece of gold film on the side of the channel, which gets bridged to the channel by the added analyte solution (Figure S19). When there is glucose in the solution, its oxidation under the catalysis of the GO enzyme will transfer electrons to the channel layer, thus de-doping the p-type conjugated polymer²⁰ (Figure 5B, right).

As shown in Figure 5C (see also Table S3), the enzyme immobilization on the semiconducting channel only causes small shift to the threshold voltage of the OECT operation in phosphate-

buffered saline (PBS) solution. The sensing performance to glucose was characterized by adding glucose in controlled concentrations into the PBS solution. When the concentration of the added glucose was equal to or greater than 1 μM , a stepwise decrease of the current was observed (Figure 5D and S20). The extent of the current decrease exhibits good correlation with the added glucose concentration (Figure 5E). In contrast, when only the PBS solution was added, there was no change in the current, suggesting the specificity to glucose as afforded by the enzyme. As a control, the device made from the pristine NHS-functionalized semiconducting film showed no response to glucose (Figure S21), which verifies that the sensing function is indeed afforded by the GO enzyme. Since the conjugation chemistry to the NHS ester group has broad applicability to other types of protein or polypeptide based bioreceptors (including both enzymes and antibodies), this material design and synthesis concept based on the CLIP method opens up the avenue of covalently functionalizing bioreceptors on mechanically soft, potentially stretchable, conjugated polymers for realizing biochemical sensing at bio-interfaces with specificity and biocompatibility.

Discussion

In summary, we established a new synthesis strategy, the CLIP method, for largely expanding the synthesizable molecular designs of conjugated polymer, towards incorporating a wide range of emerging functions. Through enabling the use of a click reaction as a post-polymerization step for the functionalization of side chains, this CLIP method is shown to be facile and highly versatile for different functional units and for both bulk and surface functionalization. This method is successfully utilized to covalently graft four different types of functional groups onto the side chains of conjugated polymers, which, otherwise, are all highly challenging to be incorporated. Two of the developed polymers are further taken to realize two highly desirable functions on conjugated polymers: direct photo-patternability, and biochemical sensing with specificity. Additional functionalities that can be incorporated by the approach can become highly valuable topics for

future investigations on the expanded uses of conjugated polymers. Through innovative incorporation of click chemistry to the design and synthesis paradigm of high-performance conjugated polymers, we anticipate that this synthesis strategy will greatly enlarge the molecular design space and thus enrich the functional properties of conjugated polymers. This will satisfy the need of their developments towards the far-reaching application area of human-integrated electronics.

Experimental procedures

Resource availability

Lead contact

Further information and requests for resources and materials should be directed to and will be fulfilled by the lead contact, Sihong Wang (sihongwang@uchicago.edu).

Materials availability

All the chemicals used in the study were purchased from Sigma-Aldrich and used without further purification. Anhydrous solvents were purchased from either Sigma-Aldrich or Fisher Scientific. 5,5'-Dibromo-3,3'-bis(2-(2-(2-methoxyethoxy)ethoxy)ethoxy)-2,2'-bithiophene was purchased from SunaTech Inc. (CAT# IN1273) and was used as received. Column chromatography was carried out with silica gel for flash chromatography from VWR Scientific. The other compounds reported in the paper can be produced following the procedures in Supplemental Information.

Data and code availability

The published article includes all data generated or analyzed during this study.

Characterizations

Microwave polymerization was conducted using a Biotage Initiator +. Nuclei magnetic resonance (NMR) spectra were recorded on a Bruker Avance III HD console spectrometer (^1H 400 MHz, ^{13}C

100 MHz) at 293 K. Chemical shifts are given in parts per million (ppm) with respect to tetramethylsilane as an internal standard, and coupling constants (J) are given in Hertz (Hz). Polymer NMR spectra were recorded at 393 K in deuterated 1,1,2,2-tetrachloroethane (TCE- d_2). High-resolution mass spectra (HR-MS) were recorded on an Agilent 6530 LC Q-TOF mass spectrometer using electrospray ionization with fragmentation voltage set at 70 V and processed with an Agilent MassHunter Operating System. Number average molecular weight (M_n), weight average molecular weight (M_w), and polydispersity index (PDI) were evaluated by high temperature size exclusion chromatography (SEC) using 1,2,4-trichlorobenzene and performed on a EcoSEC HLC-8321GPC/HT (Tosoh Bioscience) equipped with a single TSKgel GPC column (GMHHR-H; 300 mm \times 7.8 mm) calibrated with monodisperse polystyrene standards. The samples were prepared using 1 mg/mL of sample in trichlorobenzene (TCB), which were allowed to stir at 80 °C for 12 h prior to injection. The analysis of the samples was performed at 180 °C with a flow rate of 1.0 mL/min with injection quantities of 300 μ L. The data was collected and integrated using EcoSEC 8321GPC HT software suite. UV-Vis absorption spectra were recorded on the Shimadzu UV-3600 Plus UV-VIS-NIR spectrophotometer. FTIR spectra were recorded on the Shimadzu IRTracer-100 Fourier transform infrared spectrometer. Differential scanning calorimetry (DSC) experiments were performed with a TA Instruments Discovery 2500 differential scanning calorimeter. Thermal gravimetric analysis (TGA) plots were recorded with a TA Instruments Discovery thermogravimetric analyzer. The water contact angle measurement was done with a KRÜSS DSA100 drop shape analyzer. The X-ray photoelectron spectroscopy (XPS) was done with Kratos AXIS Nova with a monochromatic Al $K\alpha$ X-ray source and a delay line detector (DLD) system. Optical microscope images were captured with a Zeiss AxioScope 5/7/Vario microscope. Grazing-incidence X-ray diffraction (GIXD) was performed at the Advanced Photon Source at Argonne National Laboratory on beamline 8-ID-E⁵⁴. The X-ray energy was 10.92 keV, the incident angle was 0.14°, and the exposure time was 10 s. The area detector (Pilatus 1M, Dectris) was

translated vertically for a second exposure. The two images were combined to eliminate gaps due to rows of inactive pixels at the borders between modules using the GIXSGUI package⁵⁵ for Matlab and demonstrating that the samples were not damaged by the exposure.

Device fabrication and characterization

The thin-film transistors (TFTs) are based on bottom-contact/bottom-gate structure. The *n*-octadecyltrimethoxysilane (OTS)-treated Si/SiO₂ (300 nm) substrates⁵⁶ are cleaned by toluene. After that, the source/drain gold electrodes (50 nm) are patterned via thermal evaporation with a metal shadow mask. The channel length (*L*) and width (*W*) are 200 μm and 4 mm, respectively. The gold surface is then modified by submerging the substrates in 30 mL IPA with 10-μL 2,3,4,5,6-pentafluorothiophenol to form a SAM layer. The substrates are gently rinsed with IPA and blow-dried with nitrogen gas. The polymer solution (5 mg/mL in chlorobenzene) was then spin-coated at 1000 rpm for 60 s, followed by annealing at 150 °C for one hour in nitrogen atmosphere. All of the electrical characteristics of the semiconducting layer were measured using Keithley 4200 (Keithley Instruments Inc, Cleveland, OH, USA) under an ambient environment. The details on mobility evaluation in OTFTs are discussed in Figure S6.

The organic electrochemical transistors (OECTs) were fabricated similar to the literature previously reported⁵². Briefly, the glass substrates are cleaned with acetone, isopropyl alcohol, and water. After that, the source/drain gold electrodes (50 nm) are patterned via thermal evaporation with a metal shadow mask. The channel length (*L*) and width (*W*) are 200 μm and 4 mm, respectively. Then the polymer solution (5 mg/mL in chloroform) was spin-coated at 1000 rpm, followed by annealing at 110 °C for 30 min in nitrogen atmosphere. The electrolyte was PBS solution dropped on top of the transistors. The gate electrode was gold which was immersed in the electrolyte. The electrical characteristics of the semiconducting layer were measured using Keithley 4200 (Keithley

Instruments Inc, Cleveland, OH, USA) under an ambient environment.

Surface CLIP protocol

The surface CLIP follows the general procedure. C10-10a and C10-20a films are first spin-coated on OTS-treated silicon substrate and annealed at 150 °C for one hour. The solution of alkyne-PEG2000 (4 mg, 2 μmol) was dissolved in DMF (0.5 mL) and mixed with a solution of CuSO₄ (10 μL, 0.1 M, 1 μmol) and sodium ascorbate (20 μL, 0.1 M, 2 μmol) in water. The reaction mixture was placed on the film surface surrounded with a PDMS well and incubated at room temperature overnight. The surface was rinsed with H₂O and DMF and finally dried with nitrogen gas.

Direct photo-patterning for 10BP conjugated polymer

The C10-10BP polymer (5 mg/mL in chlorobenzene) is spin-coated on octadecyltrichlorosilane (OTS)-modified silicon oxide substrate at 1000 rpm for 60 s. The polymer film is first annealed at 140 °C for 30 minutes to remove solvent and boost the relative crystallinity. The obtained film thickness is around 30-40 nm. Then the conjugated polymer film is exposed to UV light (365 nm, 2.6 mW/cm², Spectrolinker XL-1000) with selected areas for a given period. After immersing the film in chloroform (also a good solvent for dissolving C10-10BP polymer) for 30 s with gentle shaking, the film is blow-dried by nitrogen gas, and then baked at 170 °C for 30 minutes inside glove box in order to fully remove the trapped solvent in the polymer network and further increase the relative crystallinity.

OEET glucose sensing

For the sensing experiment, glucose oxidase dissolved in PBS (pH 7.4) (3 mg/mL) was incubated on the device channel area for two hours and then rinsed with DI water. Glucose was dissolved as stock solutions in PBS. Current-voltage characteristics of the devices were recorded using a

Keithley 4200 under an ambient environment. After a steady baseline was obtained for the drain current, the glucose stock solution (4 μL each time) was injected to the electrolyte gently. For all the experiments, the volume of the electrolyte solution was kept at 0.4 mL and drain current changes in response to subsequent additions of increasing concentrations of glucose solutions into the electrolyte were monitored as a function of time.

Acknowledgments

This work is supported by the start-up fund from the University of Chicago and the US Office of Naval Research (N00014-21-1-2266). J.X. acknowledges the Center for Nanoscale Materials, a U.S. Department of Energy Office of Science User Facility, and supported by the U.S.

Department of Energy, Office of Science, under Contract No. DE-AC02-06CH11357. This research used resources of the Advanced Photon Source, a U.S. Department of Energy (DOE) Office of Science User Facility, operated for the DOE Office of Science by Argonne National Laboratory under Contract No. DE-AC02-06CH11357. S.R.-G. would like to thank the Natural Sciences and Engineering Research Council of Canada (NSERC) for financial support through a Discovery Grant (RGPIN-2017-06611) and the Canadian Foundation for Innovation (CFI).

Author contributions: N.L. and S.W. conceived and designed the experiments. N.L. synthesized and characterized the monomers and polymers. N.L., Y.D., and Y.L. fabricated the transistor devices and made the measurements. J.S., Q.Z., Y.W., and X.G. help with the GIXD characterizations. S.D., Q.S., N.O. participated the discussion of the results. B.O. and S.R.-G. performed the polymer molecular weight analysis. N.L. and S.W. co-wrote the paper. All authors reviewed and commented on the manuscript.

Competing interests: The authors declare no competing interests.

References

- 1 Yang, J., Zhao, Z., Wang, S., Guo, Y., and Liu, Y. (2018). Insight into High-Performance Conjugated Polymers for Organic Field-Effect Transistors. *Chem* 4, 2748-2785.
- 2 Li, G., Chang, W.-H., and Yang, Y. (2017). Low-bandgap conjugated polymers enabling solution-processable tandem solar cells. *Nat. Rev. Mater.* 2.
- 3 Grimsdale, A. C., Leok Chan, K., Martin, R. E., Jokisz, P. G., and Holmes, A. B. (2009). Synthesis of Light-Emitting Conjugated Polymers for Applications in Electroluminescent Devices. *Chem. Rev.* 109, 897-1091.
- 4 Neo, W. T., Ye, Q., Chua, S.-J., and Xu, J. (2016). Conjugated polymer-based electrochromics: materials, device fabrication and application prospects. *J. Mater. Chem. C* 4, 7364-7376.
- 5 Someya, T., Bao, Z., and Malliaras, G. G. (2016). The rise of plastic bioelectronics. *Nature* 540, 379-385.
- 6 Xu, J., Wang, S., Wang, G.-J. N., Zhu, C., Luo, S., Jin, L., Gu, X., Chen, S., Feig, V. R., To, J. W. F., et al. (2017). Highly stretchable polymer semiconductor films through the nanoconfinement effect. *Science* 355, 59-64.
- 7 Wang, S., Xu, J., Wang, W., Wang, G. N., Rastak, R., Molina-Lopez, F., Chung, J. W., Niu, S., Feig, V. R., Lopez, J., et al. (2018). Skin electronics from scalable fabrication of an intrinsically stretchable transistor array. *Nature* 555, 83-88.
- 8 Wang, S., Oh, J. Y., Xu, J., Tran, H., and Bao, Z. (2018). Skin-Inspired Electronics: An Emerging Paradigm. *Acc. Chem. Res.* 51, 1033-1045.
- 9 You, I., Kong, M., and Jeong, U. (2019). Block Copolymer Elastomers for Stretchable Electronics. *Acc. Chem. Res.* 52, 63-72.

- 10 Khodagholy, D., Gelinias, J. N., Thesen, T., Doyle, W., Devinsky, O., Malliaras, G. G., and Buzsaki, G. (2015). NeuroGrid: recording action potentials from the surface of the brain. *Nat. Neurosci.* *18*, 310-315.
- 11 Liu, Y., Liu, J., Chen, S., Lei, T., Kim, Y., Niu, S., Wang, H., Wang, X., Foudeh, A. M., Tok, J. B. H., et al. (2019). Soft and elastic hydrogel-based microelectronics for localized low-voltage neuromodulation. *Nat. Biomed. Eng.* *3*, 58-68.
- 12 Park, S., Heo, S. W., Lee, W., Inoue, D., Jiang, Z., Yu, K., Jinno, H., Hashizume, D., Sekino, M., Yokota, T., et al. (2018). Self-powered ultra-flexible electronics via nano-grating-patterned organic photovoltaics. *Nature* *561*, 516-521.
- 13 Dorfman, K. D., Adrahtas, D. Z., Thomas, M. S., and Frisbie, C. D. (2020). Microfluidic opportunities in printed electrolyte-gated transistor biosensors. *Biomicrofluidics* *14*, 011301.
- 14 Du, W., Ohayon, D., Combe, C., Mottier, L., Maria, I. P., Ashraf, R. S., Fiumelli, H., Inal, S., and McCulloch, I. (2018). Improving the Compatibility of Diketopyrrolopyrrole Semiconducting Polymers for Biological Interfacing by Lysine Attachment. *Chem. Mater.* *30*, 6164-6172.
- 15 Yang, Y., Liu, Z., Chen, L., Yao, J., Lin, G., Zhang, X., Zhang, G., and Zhang, D. (2019). Conjugated Semiconducting Polymer with Thymine Groups in the Side Chains: Charge Mobility Enhancement and Application for Selective Field-Effect Transistor Sensors toward CO and H₂S. *Chem. Mater.* *31*, 1800-1807.
- 16 Gasperini, A., Wang, G.-J. N., Molina-Lopez, F., Wu, H.-C., Lopez, J., Xu, J., Luo, S., Zhou, D., Xue, G., Tok, J. B. H., et al. (2019). Characterization of Hydrogen Bonding Formation and Breaking in Semiconducting Polymers under Mechanical Strain. *Macromolecules* *52*, 2476-2486.

- 17 Lin, Y. C., Chen, C. K., Chiang, Y. C., Hung, C. C., Fu, M. C., Inagaki, S., Chueh, C. C., Higashihara, T., and Chen, W. C. (2020). Study on Intrinsic Stretchability of Diketopyrrolopyrrole-Based pi-Conjugated Copolymers with Poly(acryl amide) Side Chains for Organic Field-Effect Transistors. *ACS Appl. Mater. Interfaces* *12*, 33014-33027.
- 18 Yang, Y., Liu, Z., Zhang, G., Zhang, X., and Zhang, D. (2019). The Effects of Side Chains on the Charge Mobilities and Functionalities of Semiconducting Conjugated Polymers beyond Solubilities. *Adv. Mater.* *31*, e1903104.
- 19 Tian, J., Fu, L., Liu, Z., Geng, H., Sun, Y., Lin, G., Zhang, X., Zhang, G., and Zhang, D. (2019). Optically Tunable Field Effect Transistors with Conjugated Polymer Entailing Azobenzene Groups in the Side Chains. *Adv. Funct. Mater.* *29*, 1807176.
- 20 Pappa, A. M., Ohayon, D., Giovannitti, A., Maria, I. P., Savva, A., Uguz, I., Rivnay, J., McCulloch, I., Owens, R. M., and Inal, S. (2018). Direct metabolite detection with an n-type accumulation mode organic electrochemical transistor. *Sci. Adv.* *4*, eaat0911.
- 21 Pappa, A.-M., Inal, S., Roy, K., Zhang, Y., Pitsalidis, C., Hama, A., Pas, J., Malliaras, G. G., and Owens, R. M. (2017). Polyelectrolyte Layer-by-Layer Assembly on Organic Electrochemical Transistors. *ACS Appl. Mater. Interfaces* *9*, 10427-10434.
- 22 Shen, H., Zou, Y., Zang, Y., Huang, D., Jin, W., Di, C.-a., and Zhu, D. (2018). Molecular antenna tailored organic thin-film transistors for sensing application. *Mater. Horiz.* *5*, 240-247.
- 23 Piro, B., Wang, D., Benaoudia, D., Tibaldi, A., Anquetin, G., Noel, V., Reisberg, S., Mattana, G., and Jackson, B. (2017). Versatile transduction scheme based on electrolyte-gated organic field-effect transistor used as immunoassay readout system. *Biosens. Bioelectron.* *92*, 215-220.

- 24 Khan, H. U., Roberts, M. E., Johnson, O., Forch, R., Knoll, W., and Bao, Z. (2010). In situ, label-free DNA detection using organic transistor sensors. *Adv. Mater.* *22*, 4452-4456.
- 25 Wang, Y., Gong, Q., and Miao, Q. (2020). Structured and functionalized organic semiconductors for chemical and biological sensors based on organic field effect transistors. *Mater. Chem. Front.* *4*, 3505-3520.
- 26 Pickens, C. J., Johnson, S. N., Pressnall, M. M., Leon, M. A., and Berkland, C. J. (2018). Practical Considerations, Challenges, and Limitations of Bioconjugation via Azide-Alkyne Cycloaddition. *Bioconjug. Chem.* *29*, 686-701.
- 27 Tang, W., and Becker, M. L. (2014). "Click" reactions: a versatile toolbox for the synthesis of peptide-conjugates. *Chem. Soc. Rev.* *43*, 7013-7039.
- 28 Zhang, Y., Park, A. M., McMillan, S. R., Harmon, N. J., Flatté, M. E., Fuchs, G. D., and Ober, C. K. (2018). Charge Transport in Conjugated Polymers with Pendent Stable Radical Groups. *Chem. Mater.* *30*, 4799-4807.
- 29 Chan, E. W. C., Baek, P., Barker, D., and Travas-Sejdic, J. (2015). Highly functionalisable polythiophene phenylenes. *Polym. Chem.* *6*, 7618-7629.
- 30 Hsu, L.-C., Kobayashi, S., Isono, T., Chiang, Y.-C., Ree, B. J., Satoh, T., and Chen, W.-C. (2020). Highly Stretchable Semiconducting Polymers for Field-Effect Transistors through Branched Soft–Hard–Soft Type Triblock Copolymers. *Macromolecules* *53*, 7496-7510.
- 31 Bunz, U. (2013). Adventures of an Occasional Click Chemist. *Synlett* *24*, 1899-1909.
- 32 Dorman, G., and Prestwich, G. D. (1994). Benzophenone Photophores in Biochemistry. *Biochemistry* *33*, 5661-5673.
- 33 Koniev, O., and Wagner, A. (2015). Developments and recent advancements in the field of endogenous amino acid selective bond forming reactions for bioconjugation. *Chem. Soc. Rev.* *44*, 5495-5551.

- 34 Vegas, A. J., Veiseh, O., Doloff, J. C., Ma, M., Tam, H. H., Bratlie, K., Li, J., Bader, A. R., Langan, E., Olejnik, K., et al. (2016). Combinatorial hydrogel library enables identification of materials that mitigate the foreign body response in primates. *Nat. Biotechnol.* *34*, 345-352.
- 35 Zhang, H., Li, C., Piszcz, M., Coya, E., Rojo, T., Rodriguez-Martinez, L. M., Armand, M., and Zhou, Z. (2017). Single lithium-ion conducting solid polymer electrolytes: advances and perspectives. *Chem. Soc. Rev.* *46*, 797-815.
- 36 Li, Z., Hao, P., Li, L., Tan, C. Y., Cheng, X., Chen, G. Y., Sze, S. K., Shen, H. M., and Yao, S. Q. (2013). Design and synthesis of minimalist terminal alkyne-containing diazirine photo-crosslinkers and their incorporation into kinase inhibitors for cell- and tissue-based proteome profiling. *Angew. Chem. Int. Ed. Engl.* *52*, 8551-8556.
- 37 Spicer, C. D., and Davis, B. G. (2014). Selective chemical protein modification. *Nat. Commun.* *5*, 4740.
- 38 Parker, C. G., and Pratt, M. R. (2020). Click Chemistry in Proteomic Investigations. *Cell* *180*, 605-632.
- 39 Li, N. S., Gossai, N. P., Naumann, J. A., Gordon, P. M., and Piccirilli, J. A. (2016). Efficient Synthetic Approach to Linear Dasatinib-DNA Conjugates by Click Chemistry. *Bioconjug. Chem.* *27*, 2575-2579.
- 40 Fantoni, N. Z., El-Sagheer, A. H., and Brown, T. (2021). A Hitchhiker's Guide to Click-Chemistry with Nucleic Acids. *Chem. Rev.*
- 41 Pei, D., Wang, Z., Peng, Z., Zhang, J., Deng, Y., Han, Y., Ye, L., and Geng, Y. (2020). Impact of Molecular Weight on the Mechanical and Electrical Properties of a High-Mobility Diketopyrrolopyrrole-Based Conjugated Polymer. *Macromolecules* *53*, 4490-4500.

- 42 Niu, W., Wu, H.-C., Matthews, J. R., Tandia, A., Li, Y., Wallace, A. L., Kim, J., Wang, H., Li, X., Mehrotra, K., et al. (2018). Synthesis and Properties of Soluble Fused Thiophene Diketopyrrolopyrrole-Based Polymers with Tunable Molecular Weight. *Macromolecules* *51*, 9422-9429.
- 43 Prestwich, G. D. a. G. D. (1994). Benzophenone Photophores in Biochemistry. *Biochemistry*.
- 44 Png, R. Q., Chia, P. J., Tang, J. C., Liu, B., Sivaramakrishnan, S., Zhou, M., Khong, S. H., Chan, H. S., Burroughes, J. H., Chua, L. L., et al. (2010). High-performance polymer semiconducting heterostructure devices by nitrene-mediated photocrosslinking of alkyl side chains. *Nat. Mater.* *9*, 152-158.
- 45 Kim, H. J., Han, A. R., Cho, C.-H., Kang, H., Cho, H.-H., Lee, M. Y., Fréchet, J. M. J., Oh, J. H., and Kim, B. J. (2011). Solvent-Resistant Organic Transistors and Thermally Stable Organic Photovoltaics Based on Cross-linkable Conjugated Polymers. *Chem. Mater.* *24*, 215-221.
- 46 Mueller, C. J., Klein, T., Gann, E., McNeill, C. R., and Thelakkat, M. (2016). Azido-Functionalized Thiophene as a Versatile Building Block To Cross-Link Low-Bandgap Polymers. *Macromolecules* *49*, 3749-3760.
- 47 Knopfmacher, O., Hammock, M. L., Appleton, A. L., Schwartz, G., Mei, J., Lei, T., Pei, J., and Bao, Z. (2014). Highly stable organic polymer field-effect transistor sensor for selective detection in the marine environment. *Nat. Commun.* *5*, 2954.
- 48 Palazzo, G., De Tullio, D., Magliulo, M., Mallardi, A., Intranuovo, F., Mulla, M. Y., Favia, P., Vikholm-Lundin, I., and Torsi, L. (2015). Detection beyond Debye's length with an electrolyte-gated organic field-effect transistor. *Adv. Mater.* *27*, 911-916.

- 49 Bai, L., Elosegui, C. G., Li, W., Yu, P., Fei, J., and Mao, L. (2019). Biological Applications of Organic Electrochemical Transistors: Electrochemical Biosensors and Electrophysiology Recording. *Front. Chem.* 7, 313.
- 50 Rivnay, J., Inal, S., Salleo, A., Owens, R. M., Berggren, M., and Malliaras, G. G. (2018). Organic electrochemical transistors. *Nat. Rev. Mater.* 3.
- 51 Khau, B. V., Scholz, A. D., and Reichmanis, E. (2020). Advances and opportunities in development of deformable organic electrochemical transistors. *J. Mater. Chem. C* 8, 15067-15078.
- 52 Nielsen, C. B., Giovannitti, A., Sbircea, D. T., Bandiello, E., Niazi, M. R., Hanifi, D. A., Sessolo, M., Amassian, A., Malliaras, G. G., Rivnay, J., et al. (2016). Molecular Design of Semiconducting Polymers for High-Performance Organic Electrochemical Transistors. *J. Am. Chem. Soc.* 138, 10252-10259.
- 53 Inal, S., Malliaras, G. G., and Rivnay, J. (2017). Benchmarking organic mixed conductors for transistors. *Nat. Commun.* 8, 1767.
- 54 Jiang, Z., Li, X., Strzalka, J., Sprung, M., Sun, T., Sandy, A. R., Narayanan, S., Lee, D. R., and Wang, J. (2012). The dedicated high-resolution grazing-incidence X-ray scattering beamline 8-ID-E at the Advanced Photon Source. *J. Synchrotron Radiat.* 19, 627-636.
- 55 Jiang, Z. (2015). GIXSGUI: a MATLAB toolbox for grazing-incidence X-ray scattering data visualization and reduction, and indexing of buried three-dimensional periodic nanostructured films. *J. Appl. Crystallogr.* 48, 917-926.
- 56 Chortos, A., Lim, J., To, J. W., Vosgueritchian, M., Dusseault, T. J., Kim, T. H., Hwang, S., and Bao, Z. (2014). Highly stretchable transistors using a microcracked organic semiconductor. *Adv. Mater.* 26, 4253-4259.

Figure 1. Schematic illustration of the CLIP synthetic approach, in comparison with the conventional approach, for functionalizing the side chains of conjugated polymers.

(A) Conventional method of pre-polymerization side-chain functionalization on donor-acceptor type conjugated polymers, and the associated limitations. The bold arrow at bottom right indicates the intrachain charge transport direction along the backbone.

(B) CLIP method of using CuAAC click reaction to functionalize the side chains of conjugated polymers, as a post-polymerization step. Bottom: chemical structures and the corresponding properties of the four types of functional units taken to functionalize conjugated polymers through the CLIP method.

(C) Uses of the CLIP method for two types of functionalization for conjugated-polymer thin films: the bulk functionalization by carrying out the click reaction in the solution first and then depositing the functionalized polymer into thin films; and the surface functionalization by depositing thin films from the azide-modified polymer first and then carrying out the click reaction on the film's surface.

Figure 2. Characterizations of conjugated polymers with bulk functionalization through the CLIP method.

(A) Reaction scheme for the use of the CuAAC click reaction for functionalizing four types of units on azide-functionalized DPPTT conjugated polymer, with two different alkyl linker lengths ($n = 4, 8$, respectively) and two copolymerization ratios ($y = 0.1, 0.2$, respectively) to the number of repeating units.

(B) High-temperature ^1H NMR spectra for the representative polymers before and after the click reaction. The green line labeled with a circle (\bullet) stands for the proton peak adjacent to azide group in starting polymer as indicated in (A). The green line labeled with a triangle (\blacktriangle) stands for the proton peak adjacent to triazole group in functionalized polymer as indicated in (A).

(C) OTFT device structure for charge-carrier mobility measurement.

(D) Typical transfer characteristic obtained from the functionalized polymer C10-10PY. I_d , drain current, represented by solid lines; I_g , gate current, represented by the dashed line; V_{gs} , the gate-source voltage.

(E) Typical output characteristic from C10-10PY.

(F-H) Saturation and linear charge-carrier mobilities (F), relative degrees of crystallinity and π - π spacings (extracted from GIXD measurements) (G), normalized UV-Vis absorption spectra (H), from the unfunctionalized DPPTT polymer, azide-modified polymers (C6-10a, C10-10a, C10-20a) and the further obtained PY-functionalized polymers (C6-10PY, C10-10PY, C10-20PY). C6 and C10 stand for the alkyl linker lengths of 6-carbon and 10-carbon, respectively; 10a/PY and 20a/PY stand for the side-chain modification with the azide/PY group in the molar ratio of 10 % and 20 % respectively.

(I-J) Saturation and linear charge-carrier mobilities (I), relative degrees of crystallinity and π - π spacings (extracted from GIXD measurements) (J), from the four polymers with the four functional

units functionalized on C10-10a, respectively. The error bars in **(F)** and **(I)** represent the standard deviation obtained from at least six measurements.

(K) Root-mean-square roughness of C10-10a and these four types of functionalized polymers, as determined from atomic-force microscopy (AFM) topological images.

Figure 3. Characterizations of conjugated polymers with surface functionalization through the CLIP method.

(A) Schematic images showing the process for performing the surface CLIP on a deposited film from an azide-modified conjugated polymer (i.e., C10-10a in the demonstrated experiment).

(B) Water contact angles on C10-10a film, the film modified with PEG2000 by the surface CLIP process, and the control film obtained from a C10-10a film going through the same surface CLIP process but without the Cu^I catalyst.

(C) XPS spectra showing the changes of the C 1s peaks from the three films in (B).

(D) Saturation and linear charge-carrier mobilities from C10-10a, and the functionalized polymers with PEG2000 through the surface-CLIP and the bulk-CLIP, respectively. The error bars represent the standard deviations obtained from at least six measurements.

Figure 4. Direct photo-patterning of 10BP conjugated polymer films enabled by the CLIP functionalization of benzophenone group.

(A) Schematic illustration of the UV photo-crosslinking process (365 nm) for conjugated polymer with benzophenone group.

(B) Photo-initiated interchain crosslinking reaction of the benzophenone group.

(C) Charge-carrier mobility comparison of pre-annealed (at 140 °C for 30 min), UV-exposed (365 nm, 2.6 mW/cm², for 10 minutes), and after chloroform development and post-bake (at 170 °C for 30 min). The error bars represent the standard deviation obtained from at least six measurements.

(D-E) Optical microscopy images of photo-patterned 10BP films in a “phoenix” pattern (D), and its zoom-in features (E) (scale bars: 500 μm).

Figure 5. Biochemical sensing to glucose from conjugated polymers enabled by covalent grafting of enzymatic bioreceptors.

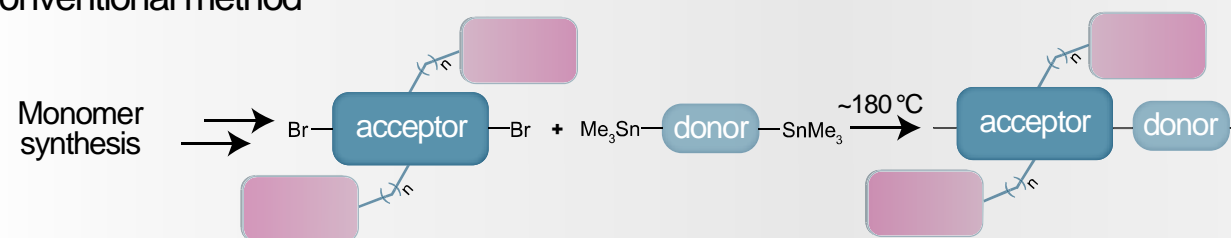
(A) Reaction scheme of the covalent bioconjugation of glucose oxidase (GO) enzyme on g2T-NHS polymer.

(B) Fabrication process of the enzymatic sensor based on OECT device design, and the recognition mechanism to glucose at the surface of the GO enzyme-modified channel layer (right). Glc: glucose; Glc-ox, glucono-1,5 lactone.

(C) Transfer curves from the OECT sensor devices with GO-enzyme-modified g2T-NHS (labeled as g2T-NHS-enzyme) and pristine g2T-NHS as the channel layer, respectively.

(D) Real-time current response ($V_{gs} = -0.2$ V, $V_{ds} = -0.05$ V) of an as-fabricated glucose sensor with g2T-NHS-enzyme to the stepwise addition of glucose in different concentrations.

(E) Drain current ($|\Delta I_d|$) response to glucose concentrations in the range of 1 μ M to 1000 μ M.

A Conventional method

- Limited functionalization
- Complicated workflow
- Sacrificed performance

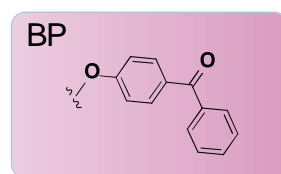
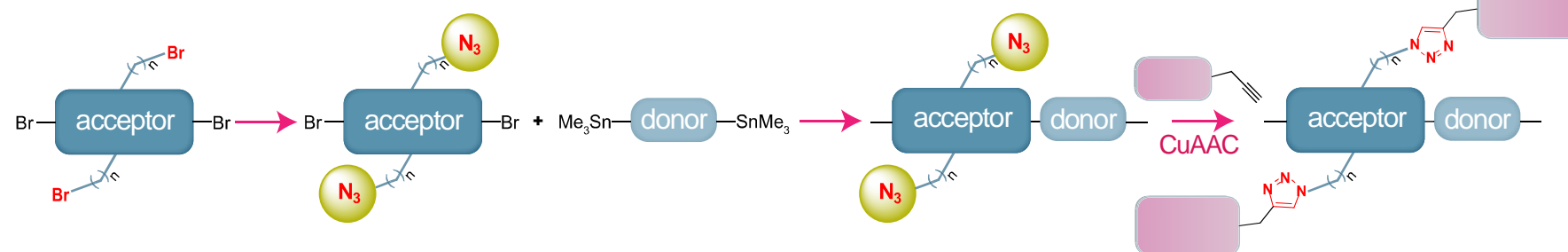
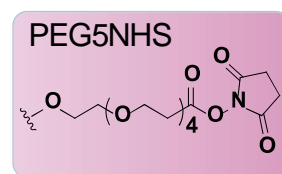
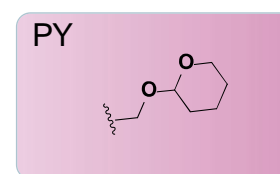
B Our method: click chemistry enabled post-polymerization functionalization (CLIP)

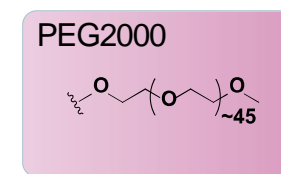
Photo-reactive



Bio-conjugatory



Immune-modulatory

Biocompatible
Ionic conducting**C**